Rotation of topological defects by trapped micro-rods in the nematic phase of a liquid crystal

DOI:
10.1016/j.molliq.2017.12.063
10.1016/j.molliq.2017.12.063

Document Version
Accepted author manuscript

Rotation of topological defects by trapped micro-rods in the nematic phase of a liquid crystal

Jiyoung Oh

Ingo Dierking*

ingo.dierking@manchester.ac.uk

School of Physics and Astronomy, University of Manchester, Oxford Road, Manchester M13 9PL, United Kingdom

*Corresponding author.

Abstract

The dynamics of rod-shaped micro-particles, trapped within a topological defect, was investigated. It is demonstrated that there is an attractive interaction force between particle and defect, which is of the order of F ≈ 30 pN, pulling the free micro-rod into the defect core, directing it along the direction of escape. Application of an electric field can induce motion of the trapped rod along the macroscopic path of a circular trajectory, which results in a circular drag motion of the defect's director field. The direction of circular motion can be clockwise or counter-clockwise with equal probability, independent of the sign of the defect. The electric field dependence of trajectory diameter and angular velocity are investigated, and it is found that these lead to a velocity, which is largely independent of electric field and particle-defect rotation direction.

Keywords: Liquid crystal; Micro-rod; Topological defect; Nematic; Electrophoresis; Particle transport

1.1 Introduction

Over the period of recent years, the introduction of nano- and micro-particles into liquid crystal phases, has become a growing field of research interest [1]. This increasing interest in dispersed systems based on anisotropic liquids is due to the vast possibilities of property manipulation offered by these materials, which can be exploited in novel applications and improved performance. Three principle directions of current efforts may be distinguished:

(i) the addition of nanoparticles, often with an added functionality such as ferroelectricity [2–4], magnetic properties [5–7] or directed conductivity like nanotubes [8–11], to a thermotropic liquid crystal. This is often nematic, but can be also be ferroelectric by itself [12–14], such as the SmC* phase, or discotic [15,16] or even lyotropic [17,18].

(ii) The formation of liquid crystalline order from anisotropic particles in isotropic solvents [19–21]. This behaviour has been demonstrated already about one century ago [22], but has largely been neglected so far, despite of the vast variety of systems available, such as inorganic liquid crystals and clays [19], biologically related nanoparticles, such as the tobacco mosaic virus, TMV, and others [22], DNA [23,24] or cellulose nanocrystals [25]. Also nanotubes and graphene oxide [26–30], as well as other micro-rod and nanowire materials can exhibit lyotropic liquid crystalline ordering.

(iii) The use of self-assembly, spontaneous ordering, and topological defects in liquid crystals to assemble nanoparticles [31–33], for example for the use as photonic materials or metamaterials, is increasingly being investigated.

It is this latter aspect that the present study is loosely related to. It is known that the introduction of particles into a uniformly aligned liquid crystal leads to the formation of defects in the vicinity of those particles [34,35]. Depending on the boundary conditions of the dispersed particle, different types of defects may be observed. There are further strong indications that dispersed particles agglomerate in and around defects of the liquid crystal director field [36–38]. Especially for the nematic phase, these defects have in turn been shown to interact, with defects of equal strength but opposite sign attracting each other and annihilating in a process called the Kibble-Zurek mechanism [39–43]. At last, it has been observed that dispersed particles can be transported through the liquid crystal medium (and also the liquid phase), by application of alternating electric fields. This has been demonstrated in the nematic [44], the ferroelectric smectic C* [45], the chiral nematic [46] and the isotropic phase and is attributed to electrophoresis. In contrast to common liquids, the liquid crystal environment gives rise to a variety of novel particle transport properties. The current state of knowledge has been summarized in an excellent review by Lavrentovich [47]. Particle transport occurs only above a certain electric field threshold, which is dependent on the applied frequency. Several different modes of particle motion can be observed in the field amplitude-frequency, (E,f)-parameter space. For micro-particles of spherical symmetry, several different modes of particle transport have been observed: (i) no motion below a frequency dependent threshold voltage. (ii) linear particle displacement in a direction perpendicular to the applied electric field direction. (iii) micro-sphere motion along a circular trajectory in a plane normal to the electric field vector. This is not due to the twist escape structure between two defects of opposite sign, as the circular motion is also observed for uniformly oriented liquid crystals and even for the isotropic phase [46,47]. It is believed to be

related to electrophoresis. Finally, (iv) random motion for large applied electric fields, which is due to electro-hydrodynamic flow, and which generally represents the upper limit of investigation shortly before dielectric breakdown.

These types of transport are observed for spherically symmetric particles, while rod-like particles, like they are used in the present investigation, show a much more complex behaviour with additional internal degrees of motion, such as rotations around the long and short axes. In this study, we will combine several of the above outlined aspects, such as particle trapping in defects and particle transport in liquid crystals, in an investigation that describes particle mediated defect transport.

~~2.~~2 Experimental

The investigations were carried out by employing a commercially available, room temperature liquid crystal mixture, ZLI-2806, from Merck, Darmstadt, which was used as provided. The liquid crystal has a phase sequence on cooling of Iso 100 N ~~-~~ 20 Cryst. (temperatures in ~~oC~~°C), and exhibits a negative dielectric anisotropy $\Delta\varepsilon < 0$. The dispersed silica micro-rods were standard spacer rods as used in sandwich cell or display production (PF-15S, Nippon Electric Glass, kindly provided by Uros Tkalec), with a monodisperse width of 1.5 µm, while the length varied between approximately 5-10 µm, averaging at 8.3 µm. They were dispersed in the liquid crystal at minute amounts, such that the particle density was extremely low. This is of importance, as due to the elastic properties of the liquid crystal, the flow fields created during the motion of individual particles may easily influence the motion of other particles in their vicinity. Due to the small diameter of the rods, it is hard to visualize the director configuration around the rods, but comparison with images by Tkalec et al. [48], it appears that the boundary conditions on the rods are homeotropic and leading to a dipolar defect configuration.

Standard sandwich cells of thickness 10 µm and homeotropic boundary conditions were filled by capillary action, and investigated at room temperature in the nematic phase. All investigations were performed with external electric fields applied. This implies that due to the negative dielectric anisotropy the video recordings and the measurements were done at planar orientation of the liquid crystal, despite the homeotropic substrate boundary conditions. This procedure was necessary in order to induce the umbilic defects in the nematic director field.

Time resolved image acquisition in polarized microscopy (POM) was employed to extract the motion of particles. A polarizing microscope (Leica OPTIPOL) was equipped with a digital camera (uEye Gigabit Ethernet UI-5460-C), which was linked to image capture software. The camera frame rate was 56 images per second, of which every second image was extracted from the movies. The time resolution was thus 0.035 s. The spatial resolution of the camera was 1000~~x~~ × 720 pixel. Square wave alternating electric fields were applied by a function generator (TTi TG1010) in combination with an in-house built power amplifier to induce micro-rod motion. Subsequent image analysis was carried out with software ImageJ, developed at the National Institutes of Health, Maryland, USA.

~~3.~~3 Experimental ~~R~~results and ~~D~~discussion

For cylinder-like, rod-shaped micro-particles, the following qualitative types of motion can specifically be observed: (a) the rotation in the plane of the substrates around the short cylinder axis, which points along the applied electric field, and thus perpendicular to the substrate plane. One can also observe (b) a rotation around the perpendicular short axis, which lies in the substrate plane, thus perpendicular to the electric field vector. It is not clear if there is (c) also a possible rotation around the cylinder's long axis, (may this point along or perpendicular to the applied field direction), because this would be extremely hard to be resolved by optical microscopy. It should also be pointed out, that the translational modes can be superimposed by the rotational ones. One can thus for example observe instances where a micro-rod rotates around its short axis, while moving on a macroscopic circular or linear trajectory.

While these complex combinations are currently subject to detailed quantitative investigations, we will here discuss a slightly different but nonetheless intriguing scenario, involving cylindrical micro-particles in combination with defects. Fig~~ure~~. 1 schematically depicts the situation as a side view of the employed sandwich cells. The umbilic defect is indicated as a director field, which at the point of singularity escapes into the third dimension, where the director is practically undefined. These defects are generally observed when a nematic liquid crystal with negative dielectric anisotropy is switched from homeotropic to planar orientation when applying an electric field.

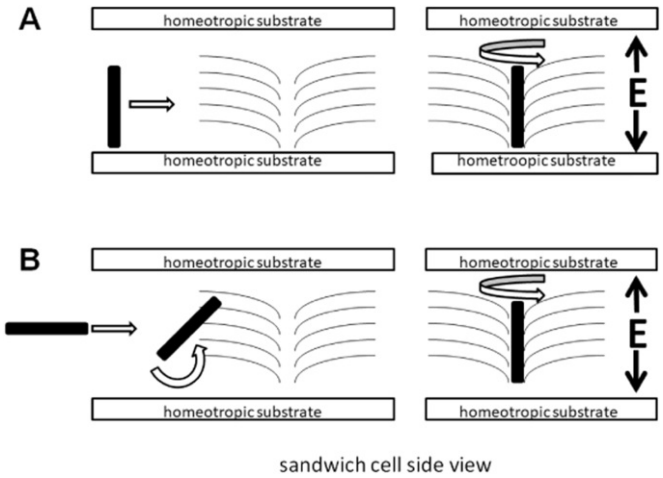

~~Figure 1.~~Fig. 1 Schematic side view of a liquid crystal sandwich cell with a topological defect whose core escapes into the third dimension. A suspended micro-rod is attracted towards the core, where in case A) it already exhibits the correct orientation, while in case B) it will be rotated towards the direction of escape. Eventually being trapped within the defect core and with an alternating electric field applied, the micro-rod can undergo translational and rotational motion along different macroscopic trajectories.

alt-text: Fig. 1

Two cases, which are very similar and eventually result in the same configuration, can be observed. In case A) the micro-rod is already oriented perpendicular to the bounding substrates, thus along the core of the defect. The particle is attracted towards the defect core and is eventually trapped (see Movie (1), slowed down by a factor 8 from real time). This is the case presented below. Indeed, the trapping force is quite strong, because the particle will not leave the defect again. This is believed to be due to a minimization of the elastic free energy density, as the micro-rod takes up the role of the director field distortion. Not pictured, but nevertheless observed qualitatively, was also case B) where the micro-rod is initially oriented perpendicular to the defect core, thus parallel to the bounding substrates. As the rod is attracted into the core, it is rotated by 90 degrees, so that it fills up an as large as possible portion of the defect core. The particle thus ends in the same situation as for case A), and in both cases, the micro-rod can then be seen to proceed on a circular trajectory, dragging the whole defect and its director field with it, as shown in Movie (2).

Fig~~ure~~. 2 illustrates by micro-photographs the approach of the micro-rod towards the defect core as outlined for case A). While the defect remains practically stationary within the limits of experimental error, the micro-rod is attracted to it and moves on a linear trajectory and at a constant speed of approximately $\sim 30\,\mu m\,s^{-1}$ directly into the core. The whole process, as shown in Fig~~figure~~. 2(A)–(I) takes a time period of about 0.3 s, and is graphically depicted as trajectories in Fig~~figure~~. 3(A). A more detailed analysis, determining the distance between micro-rod particle and defect core as a function of time to fusion shows that the motion is linear, in contrast to the square-root behaviour observed in defect annihilation processes. It is not quite clear why the observed motion is in fact linear, with a constant speed, as this behaviour is normally only observed at large separations, for example between two defects of opposite sign, changing to a square-root behaviour close before annihilation [43]. One reason may be that in this case the nonlinear regime, shortly before the rod merges with the defect core, is too small to be resolved with the employed experimental setup. But possibly the here described experiment is in fact different from defect annihilation experiments. It is worthwhile to point out that the determined particle velocity towards the defect is equivalent to recently determined values in the defect annihilation process between two defects at approximately the same separation [49], which was in the limit of large separation distances. By using the determined velocity $v \approx 30\,\mu m\,s^{-1}$, diameter $d \approx 1.5\,\mu m$ and length $l \approx 8\,\mu m$ of the micro-rod, and a typical nematic viscosity of $\eta \approx 70\,mPa \cdot s$ [50], we estimate the force F between the colloidal micro-rod and the defect to be in the range of $F \approx 30\,pN$, assuming an attractive force equal to a Stokes drag force, slightly modified for the cylinder particle geometry. The micro-rod, suspended in the nematic liquid crystal, gives rise to defects in its very close vicinity, which interact with other defects. It is equivalent for the latter to be generated macroscopically in a director field as in this case, or by other particles, which leads to the often observed chaining [48,7] or the possibility to produce defect mediated colloidal crystals [31,32].

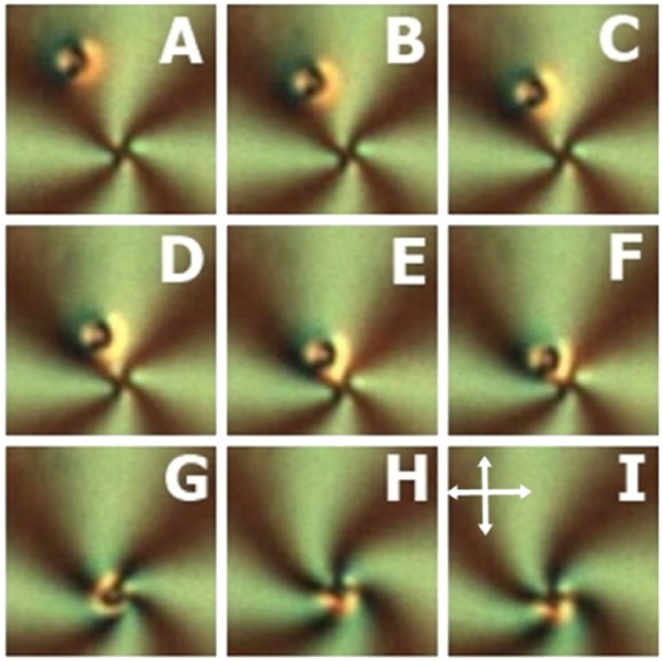

~~Figure 2:~~Fig. 2

Time series of the micro-rod being attracted by the four-brushed defect of strength | s | = 1, approaching the defect (A)–(F) and being trapped (G)–(I). Comparison of the images of the rod with those presented in [48], suggest a dipolar defect arrangement, thus hometropic anchoring of the director on the micro-rods. The images are spaced equally in time, with the whole sequence being approximately 0.3 s. The image size is approximately 20~~*~~ × 20 µm (see also Movie (1)).

alt-text: Fig. 2

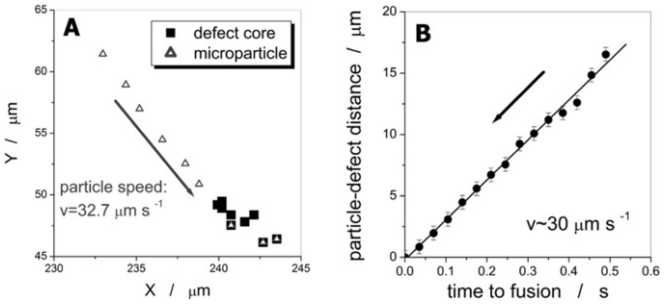

~~Figure 3:~~Fig. 3 (A) Micro-rod (open triangles) approaching the practically stationary defect (closed squares) on a linear trajectory, due to the attractive force between rod and defect. (B) From the constant micro-rod motion a linear speed of approximately $v \approx 30\ \mu m\ s^{-1}$ can be determined.

alt-text: Fig. 3

The actual macroscopic motion of the standing up micro-rod on a circular trajectory is exemplary demonstrated by the texture time series of Fig~~figure~~. 4(A)–(I). The time difference between each micrograph is approximately ~ 0.35 s. Movie (2) provides the corresponding dynamic, visual impression. The movie is slowed down by a factor 8 in comparison to real time.

Measurements of the circular motion were carried out as a function of applied electric field of $E = 2$, 3, 4, and $5\ MV\ m^{-1}$. The lowest electric field of $E = 2\ MV\ m^{-1}$ is only slightly above the threshold for circular particle motion. Analysing every 10th frame of the corresponding movies, the actual trajectories can be plotted out in the X-Y plane, which is equivalent to the substrate plane, and therefore perpendicular to the direction of the applied electric

field vector, as shown in Figfigure. 5. The indicated circles are a guide to the eye for judgement of the closeness of the trajectory to a circular path.

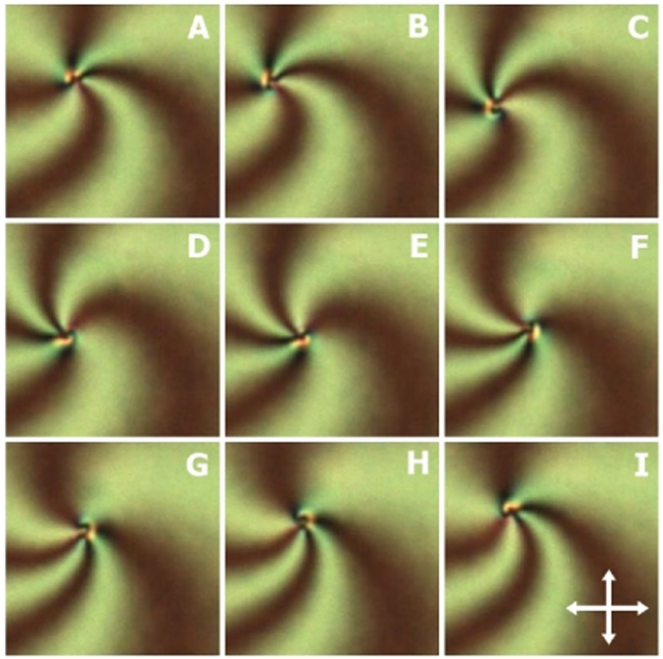

~~Figure 4.~~Fig. 4

Exemplary time series of the defect-trapped micro-rod describing a circular trajectory in the plane of the substrate, perpendicular to the applied electric field. The trapped rod does not escape the defect and thus drags it along its circular path (see als Movie (2)). The time laps between each image ~~is~~ are about 0.35 s, and the image size is approximately 50~~x~~ × 50 µm.

alt-text: Fig. 4

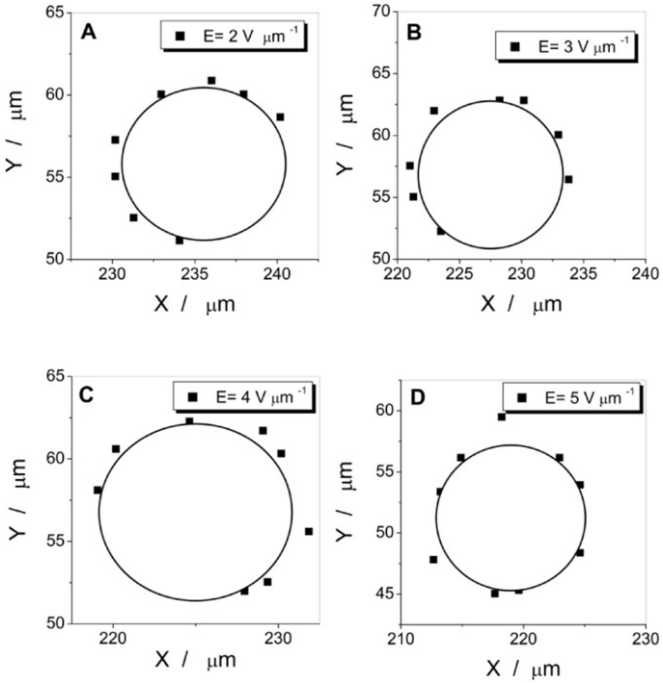

~~Figure 5.~~Fig. 5 Plots of the spatial micro-rod/defect positions as a function of time, illustrating the circular trajectory, which is indicated as a guide to the eye for easy judgement of the path. Measurements are presented for different applied electric field amplitudes. A: $E = 2\ MV\ m^{-1}$, just above the threshold for circular particle motion, B–D: $E = 3, 4, 5\ MV\ m^{-1}$, respectively.

alt-text: Fig. 5

From Fig~~ure~~. 5(B)–(D) it can be concluded that the diameter of the circular trajectory is within experimental error practically constant with increasing applied electric field amplitude (see Fig~~ure~~. 6(A)). The angular velocity ω of the particle, and thus the whole defect being dragged in the plane of the substrates also appears to be largely unaffected with increasing applied electric field amplitude, within the limitations of experimental errors (see Fig~~ure~~. 6(B)). It should be pointed out that only few measurements could be taken, and that a variation of about 25% of the measured values of diameter and angular velocity at $E = 2\ MV\ m^{-1}$, close to the threshold voltage of $E_{th} = 1.5\ MV\ m^{-1}$, would in fact display a trend as it has been observed for spheres in the isotropic phase, with a decreasing diameter and increasing angular velocity for increasing electric field amplitude [46]. The measurements presented here do carry a relatively large error, which is most likely due to the mutual influence of the flow fields created by defects and other particles in the vicinity.

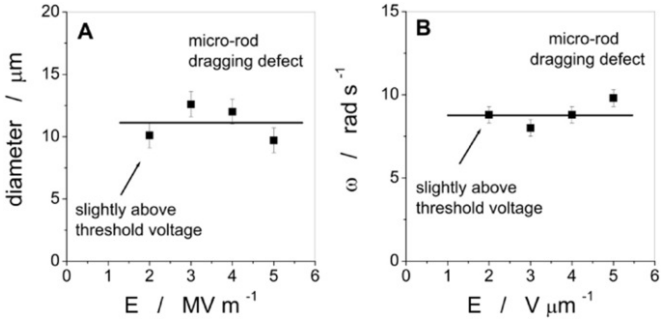

~~Figure 6.~~Fig. 6 Electric field amplitude dependence of A: the diameter and B: the angular velocity of the micro-rod/defect system moving on the circular trajectory.

alt-text: Fig. 6

At this point it should be noted that the directionality of rotational movement of simple spherical micro-particles in a defect-free nematic phase occurs clockwise and counter-clockwise with the same probability. This is the same for micro-rods trapped in a | s |=1 defect, which are the only ones observed when generated by electric field application (umbilics). Furthermore, the rotation direction of the micro-rod, and therefore that of the defect, is also not related to the sign of the defect strength. This is demonstrated by Movie (3), which is slowed down by a factor 4 in comparison to real time, and as a time series of textures in Fig~~figure~~. 7.

The two defects that are containing a trapped micro-rod each, are highlighted by arrows in Fig~~figure~~. 7(A). One of them rotates clockwise, while the other rotates counter-clockwise. The network of defects induced by the application of an electric field, contains only defects of strength s = ± 1, and always connects defects of opposite sign. Thus, the micro-rod trapped defect on the left is connected to one of opposite sign seen at the top and the bottom in the figures. This implies that the micro-rod trapped defect in the right of the figure has the same sign, and thus director configuration, as that to the left. Nevertheless, as can be seen from Figs~~figures~~. 7(A)-(L), both micro-rod trapped defects rotate in opposite directions.

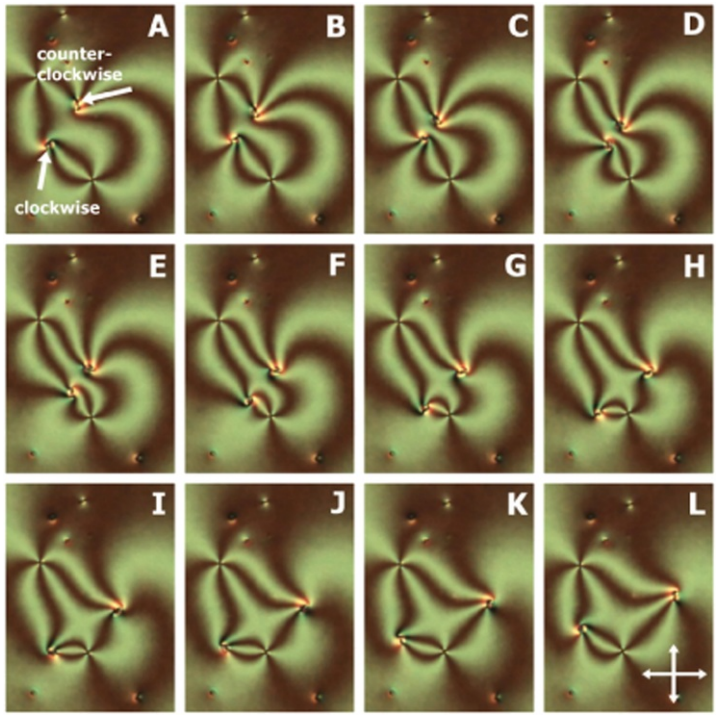

~~Figure 7:~~Fig. 7

Time series of two micro-rods trapped in defects of equal strength at the same time, moving on a circular path in opposite directions, as indicated in part A. The images are equally spaced in time and the complete sequence has a time period of 4.3 s (see also Movie (3)). The image size is approximately 40~~x~~ × 50 µm, E = 2 MV m^{-1}.

alt-text: Fig. 7

To quantify this behaviour further, Fig~~figure~~. 8 depicts the trajectories of the two micro-rods moving on a circular path, while dragging the trapped defects with them. Despite the fact that the two defects are clearly interacting with each other, the trajectory of the micro-rods still very much describes a circle, as illustrated in Fig~~figure~~. 8 by the guide to the eye. Investigating the actual diameters of the circular paths, one finds that ~~that~~ of the clockwise rotating defect is d = 10 µm, while the counter-clockwise moving defect describes a circular path with diameter d = 18 µm. Clockwise and counter-clockwise path differ in diameter by a factor of two. At the same time, the clockwise moving defect exhibits an angular velocity of ω = 1.46 rads^{-1}, while its counterpart is travelling at ω = 0.73 rads^{-1}, again approximately a factor of two difference. This implies, that the linear speed v = ωR, with R the radius of the circular trajectory, of both micro-rods, and therefore dragged defects, is constant at v = 7 µm s^{-1}, independent of the rotation direction, and equal for defects of the same sign, in contrast to defect annihilation dynamics between defects of opposite sign translate at different speeds [43].

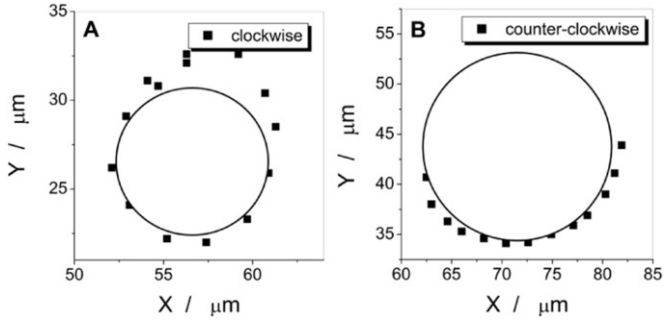

~~Figure 8.~~ Fig. 8

Graphic representation of the information contained in the image series of Fig~~figure~~. 7 (Movie (3)), illustrating that both the clockwise and the counter-clockwise moving micro-rod/defect pair are still following a circular trajectory, despite their mutual interaction. The clockwise trajectory has only half of the diameter of the counter-clockwise one, while the speed of the former is twice as large as that of the latter, again indicating a constant linear speed of the micro-rod. The applied field amplitude was $E = 2\,MV\,m^{-1}$. Circles are a guide to the eye to judge the particle trajectory.

alt-text: Fig. 8

~~4.~~4 Conclusions

Micro-rods of cylindrical symmetry can be trapped along the escape direction of nematic topological defects. An attractive force of the order of $F \approx 30$ pN acts between particle and defect, which is due to the interaction between the defect in the macroscopic director field, and that generated by the presence of the colloidal particle. Application of an alternating electric field can cause the micro-rod to describe a path along a circular trajectory, dragging the associated topological defect with it. In the present study, which was limited to a relatively small variation regime of the applied electric field strength, the diameter and angular velocity of the circular defect motion appears to be constant within the limits of errors. The rotation direction of defects of equal strengths can be clockwise as well as counter-clockwise, implying that the director distribution around the defect does not predetermine the rotation direction.

Supplementary data to this article can be found online at https://doi.org/10.1016/j.molliq.2017.12.063.

References

[1] J.P.F. Lagerwall and G. Scalia, (Eds.), *Liquid Crystals with Nano and Microparticles,* 2017, World Scientific; Singapore.

[2] Y. Reznikov, O. Buchnev, O. Tereshchenko, V. Reshetnyak, A. Glushchenko and J. West, *Appl. Phys. Lett.* **82**, 2003, 1917.

[3] F.H. Li, J. West, A. Glushchenko, C. Il Cheon and Y. Reznikov, *J. Soc. Inf. Disp.* **14**, 2006, 523.

[4] S. Al-Zangana, M. Turner and I. Dierking, *J. Appl. Phys.* **121**, 2017, 085105.

[5] N. Podoliak, O. Buchnev, O. Buluy, G. D'Alessandro, M. Kaczmarek, Y. Reznikov and T.J. Sluckin, *Soft Matter* **7**, 2011, 4742.

[6] A. Mertelj, D. Lisjak, M. Drofenik and M. Copic, *Nature* **504**, 2013, 237.

[7] I. Dierking, M. Heberle, M.A. Osipov and F. Giesselmann, *Soft Matter* **13**, 2017, 4636.

[8] I. Dierking, G. Scalia, P. Morales and D. LeClere, *Adv. Mater.* **16**, 2004, 865.

[9] I. Dierking, G. Scalia and P. Morales, *J. Appl. Phys.* **97**, 2005, 044309.

[10] J.P.F. Lagerwall and G. Scalia, *J. Mater. Chem.* **18**, 2008, 2890.

[11] S.P. Yadav and S. Singh, *Prog. Mater. Sci.* **80**, 2016, 38.

[12] F.V. Podgornov, A.M. Suvorova, A.L. Lapanik and W. Haase, *Chem. Phys. Lett.* **479**, 2009, 206.

[13] J. Prakash, A. Choudhary, D.S. Metha and A.M. Biradar, *Phys. Rev. E* **80**, 2009, 012701.

[14] M. Yakemseva, I. Dierking, N. Kapernaum, N. Usoltseva and F. Giesselmann, *Eur. Phys. J. E* **37**, 2014, https://doi.org/10.1140/epje/i2014-14007-4.

[15] S. Kumar and H.K. Bisoyi, *Angew. Chem. Int. Ed.* **46**, 2007, 1501.

[16] H.K. Bisoyi and S. Kumar, *J. Mater. Chem.* **18**, 2008, 3032.

[17] J. Lagerwall, G. Scalia, M. Haluska, U. Dettlaf-Weglikowska, S. Roth and F. Giesselmann, *Adv. Mater.* **19**, 2007, 359.

[18] W. Jiang, B. Yu, W. Liu and J. Hao, *Langmuir* **23**, 2007, 8549.

[19] A.S. Sonin, *J. Mater. Chem.* **8**, 1998, 2557.

[20] J.C.P. Gabriel and P. Davidson, Colloid Chemistry 1 in Topics in Current Chemistry, **226**, 2003, 119.

[21] I. Dierking and S. Al-Zangana, Nanomaterials, 2017, (submitted).

[22] H. Diesselhorst and H. Freundlich, *Phys. Z.* **16**, 1915, 419.

[23] T.E. Strzelecka, M.W. Davidson and R.L. Rill, *Nature* **331**, 1988, 457.

[24] F. Livolant and A. Leforestier, *Prog. Polym. Sci.* **21**, 1996, 1115.

[25] X.M. Dong, T. Kimura, J.F. Revel and D.G. Gray, *Langmuir* **12**, 1996, 2076.

[26] W. Song, I.A. Kinloch and A.H. Windle, *Science* **302**, 2003, 1363.

[27] S. Badaire, C. Zakri, M. Maugey, A. Derre, J.N. Barisci, G. Wallace and O. Poulin, *Adv. Mater.* **13**, 2005, 1673.

[28] J.E. Kim, T.H. Han, S.H. Lee, J.Y. Kim, C.W. Ahn, J.M. Yun and S.O. Kim, *Angew. Chem. Int. Ed.* **50**, 2011, 3043.

[29] Z. Xu and C. Gao, *Nature Comm.* **2**, 2011, 571, (DOI: 10.1038.ncomm1583).

[30] S. Al-Zangana, M. Iliut, M. Turner, A. Vijayaraghavan and I. Dierking, 2D, *Dent. Mater.* 2017, (in press).

[31] I. Musevic, M. Skarabot, U. Tkalec, M. Ravnik and S. Zumer, *Science* **313**, 2006, 954.

[32] I. Musevic and M. Skarabot, *Soft Matter* **4**, 2008, 195.

[33] I. Musevic, *Liq. Cryst. Rev.* **4**, 2016, 1.

[34] P. Poulin, H. Stark, T.C. Lubensky and D.A. Weitz, *Science* **275**, 1997, 1770.

[35] H. Stark, *Eur. J. Phys. B* **10**, 1999, 311.

[36] I. Dierking, W. Blenkhorn, E. Credland, W. Drake, R. Kociuruba, B. Kayser and T. Michael, *Soft Matter* **8**, 2012, 4355.

[37] A.C. Pawsey, J.S. Lintuvuori, T.A. Wood, J.H.J. Thijssen, A. Marenduzzo and P.S. Clegg, *Soft Matter* **8**, 2012, 8422.

[38] A.C. Pawsey and S. Clegg, *Soft Matter* **11**, 2015, 3304.

[39] I. Chuang, B. Yurke, R. Durrer and N. Turok, *Science* **251**, 1991, 1336.

[40] A. Pargellis, N. Toruk and B. Yurke, *Phys. Rev. Lett.* **67**, 1991, 1570.

[41] I. Chuang, B. Yurke, A.N. Pargellis and N. Toruk, *Phys. Rev. E* **47**, 1993, 3343.

[42] I. Dierking, O. Marshall, J. Wright and N. Bulleid, *Phys. Rev. E* **71**, 2005, 061709.

[43] I. Dierking, M. Ravnik, E. Lark, J. Healey, G.P. Alexander and J.M. Yeomans, *Phys. Rev. E* **85**, 2012, 021703.

[44] I. Dierking, G. Biddulph and K. Matthews, *Phys. Rev. E* **73**, 2006, 011702.

[45] I. Dierking, P. Cass, K. Syres, R. Cresswell and S. Morton, *Phys. Rev. E* **76**, 2007, 021707.

[46] J. Oh, H.F. Gleeson and I. Dierking, *Phys. Rev. E* **95**, 2017, 022703.

[47] O.D. Lavrentovich, *Soft Matter* **10**, 2014, 1264.

[48] U. Tkalec, M. Skarabot and I. Musevic, *Soft Matter* **4**, 2008, 2402.

[49] M. Nikkhou, M. Skarabot and I. Musevic, *Phys. Rev. E* **93**, 2016, 062703.

[50] A.G. Chmielewski, *Mol. Cryst. Liq. Cryst.* **132**, 1986, 339.

E-Extra

Time series of the micro-rod being attracted by the four-brushed defect of strength | s |=1, approaching the defect (A)-(F) and being trapped (G)-(I). Comparison of the images of the rod with those presented in [48], suggest a dipolar defect arrangement, thus hometropic anchoring of the director on the micro-rods. The images are spaced equally in time, with the whole sequence being approximately 0.3 s. The image size is approximately 20~~x~~ × 20 µm (see also Movie (1)).

Exemplary time series of the defect-trapped micro-rod describing a circular trajectory in the plane of the substrate, perpendicular to the applied electric field. The trapped rod does not escape the defect and thus drags it along its circular path (see also Movie (2)). The time laps between each image ~~is~~ are about 0.35 s, and the image size is approximately 50~~x~~ × 50 µm.

Time series of two micro-rods trapped in defects of equal strength at the same time, moving on a circular path in opposite directions, as indicated in part A. The images are equally spaced in time and the complete sequence has a time period of 4.3 s (see also Movie (3)). The image size is approximately 40~~x~~ × 50 µm, $E = 2\ MV\ m^{-1}$.

Graphic representation of the information contained in the image series of Fig~~figure~~ 7 (Movie (3)), illustrating that both the clockwise and the counter-clockwise moving micro-rod/defect pair are still following a circular trajectory, despite their mutual interaction. The clockwise trajectory has only half of the diameter of the counter-clockwise one, while the speed of the former is twice as large as that of the latter, again indicating a constant linear speed of the micro-rod. The applied field amplitude was $E = 2\ MV\ m^{-1}$. Circles are a guide to the eye to judge the particle trajectory.

Two cases, which are very similar and eventually result in the same configuration, can be observed. In case A) the micro-rod is already oriented perpendicular to the bounding substrates, thus along the core of the defect. The particle is attracted towards the defect core and is eventually trapped (see Movie (1), slowed down by a factor 8 from real time). This is the case presented below. Indeed, the trapping force is quite strong, because the particle will not leave the defect again. This is believed to be due to a minimization of the elastic free energy density, as the micro-rod takes up the role of the director field distortion. Not pictured, but nevertheless observed qualitatively, was also case B) where the micro-rod is initially oriented perpendicular to the defect core, thus parallel to the bounding substrates. As the rod is attracted into the core, it is rotated by 90 degrees, so that it fills up an as large as possible portion of the defect core. The particle thus ends in the same situation as for case A), and in both cases, the micro-rod can then be seen to proceed on a circular trajectory, dragging the whole defect and its director field with it, as shown in Movie (2).

The actual macroscopic motion of the standing up micro-rod on a circular trajectory is exemplary demonstrated by the texture time series of Fig~~figure~~ 4(A)-(I). The time difference between each micrograph is approximately ~ 0.35 s. Movie (2) provides the corresponding dynamic, visual impression. The movie is slowed down by a factor 8 in comparison to real time.

At this point it should be noted that the directionality of rotational movement of simple spherical micro-particles in a defect-free nematic phase occurs clockwise and counter-clockwise with the same probability. This is the same for micro-rods trapped in a | s |=1 defect, which are the only ones observed when generated by electric field application (umbilics). Furthermore, the rotation direction of the micro-rod, and therefore that of the defect, is also not related to the sign of the defect strength. This is demonstrated by Movie (3), which is slowed down by a factor 4 in comparison to real time, and as a time series of textures in

Fig~~figure~~. 7.

E-component

The following are the supplementary data related to this article.

Multimedia Component 1 

Supplementary video 1

alt-text: Supplementary video 1

Multimedia Component 2 

Supplementary video 2

alt-text: Supplementary video 2

Multimedia Component 3 

Supplementary video 3

alt-text: Supplementary video 3

Highlights

- Demonstration of defect trapping of micro-rod particles in liquid rystals
- Estimation of attractive force between particle and defect to F ~ 1 pN
- First demonstration of regular defect dragging on circular trajectory by moving micro-rod
- Demonstration of independence of motion on defect sign
- First detailed study of rod-like particle electrophoresis in liquid crystals

---

Queries and Answers

Query:

Your article is registered as belonging to the Special Issue/Collection entitled “Prof. Yuriy Reznikov”. If this is NOT correct and your article is a regular item or belongs to a different Special Issue please contact santhoshi.bs@elsevier.com immediately prior to returning your corrections.

Answer: This is correct. But the first author, Jiyoung Oh, would like to add the following: present address: College of Pharmacy, Hanyang University, 222 Wangsimni-ro, Sageun-dong, Seongdong-gu, Seoul, South Korea.

Query:

Please confirm that given names and surnames have been identified correctly and are presented in the desired order, and please carefully verify the spelling of all authors’ names.

Answer: Yes.

Query:

The author names have been tagged as given names and surnames (surnames are highlighted in teal color). Please confirm if they have been identified correctly.

Answer: Yes

Query:

Please provide caption for Supplementary video 1.

Answer: Micro-rod attracted by defect

Query:

Please provide caption for Supplementary video 2.

Answer: Circular defect trajectory caused by trapped micro-rod.

Query:

Please provide caption for Supplementary video 3.

Answer: Defect pair rotation.

Query:

Please provide an update for reference “[30]”.

Answer: S. Al-Zangana, M. Iliut, M. Turner, A. Vijayaraghavan, I. Dierking, 2D Mater., **4**, (2017), 041004